AN ECG ARTIFACT REDUCTION METHODOLOGY BASED ON PARAMETER ADAPTATION OF ANALOG FILTERS

Paul FARAGÓ , Claudia FARAGÓ , Sorin HINTEA
Technical University of Cluj-Napoca, Bases of Electronics Department, Romania
Str. Bariţiu 26-28, 400027 Cluj-Napoca, Phone: +40 264 401463, Fax: +40 264 591340, Paul.Farago@bel.utcluj.ro

Abstract: Portable and wearable bio-medical monitoring systems operate towards in-vivo acquisition and analysis of bio-potentials in ubiquitous healthcare. A challenge which needs to be addressed is artifact suppression. This article proposes a solution for electrocardiogram (ECG) artifact reduction via tunable analog filtering. An electronically tunable operational transconductance amplifier was developed to implement a Kerwin-Huelsman-Newcomb (KHN) biquad. A filter parameter adaptation methodology was implemented on a feed-forward control loop, to determine the filtering characteristics for frames of ECG signal. Simulation results validate the proposed methodology for ECG artifact reduction.

Keywords: *ECG analog front-end, operational amplifiers, Kerwin-Huelsman-Newcomb (KHN) biquad, feed-forward control, parameter adaptation.*

I. PAGE FORMAT

Biomedical monitoring systems operate towards the in-vivo acquisition and monitoring of the human body bio-potentials, e.g. electrocardiogram (ECG), electromiogram (EMG), electroencephalogram (EEG), etc. [1, 2]. Latest trends in the field of biomedical electronics targets the development of battery-operated, or even battery-less wearable devices to enable portability and autonomy of the medical equipment, and consequently insure patient comfort [3]. Indeed, healthcare currently undergoes the transition from hospital-centered towards a ubiquitous monitoring environment [4]. Thus, wearable monitoring systems are proven to be particularly useful in ubiquitous healthcare, providing consistent support for patient supervision and enabling an early diagnosis outside the hospital.

In hospital environment, bio-potential monitoring is performed with standard procedures. Wearable monitoring devices in ubiquitous healthcare on the other hand raise several challenges coming from patient continuous movement, improper attachment of the electrodes, loose conductors, etc. This affects the biomedical signal by a wide range of artifacts: power line interference, electrode contact noise, motion artifacts, muscle contractions and baseline wander [4, 5]. The artifacts are characterized in terms of amplitude, duration and frequency in table 1 [5, 6].

Artifacts manifest in an additive manner, thus distorting the features of the biomedical signal and disturbing the diagnostic process. Motion artifacts for example, which exhibit rather large amplitudes within the frequency band of interest, are superimposed to the biomedical signal, corrupting its shape. Another very common example is the interaction among different biomedical signals, e.g. the EMG from respiration and muscle contractions is superimposed over the ECG, eye movement is superimposed over the EEG, etc. [6].

The most common approach for artifact removal is filtering. A challenge in artifact removal however comes from the requirement to identify the filter parameters. Low-frequency artifacts, such as baseline wander, are suppressed with a highpass filter (HPF). High-frequency artifacts on the other hand, such as interferences with EMG or EEG, are suppressed with a lowpass filter (LPF). Power line interference is suppressed with notch filtering. The problem which has to be solved is to determine the optimal value of the filter cutoff frequencies, which will vary in time as a result of the time varying nature of biomedical signals [6].

Table 1. Biomedical signal artifact characteristics

Artifact	Amplitude	Duration	Frequency
Stray interference	50% of V_{ECG}^{p-p}	continuous	High frequency
Power line interference	50% of V_{ECG}^{p-p}	continuous	50 Hz
Electrode contact noise	max	1 sec	60 Hz
Motion artifacts	500% of V_{ECG}^{p-p}	100-500 ms	High frequency
Muscle contractions	10% of V_{ECG}^{p-p}	50 ms	DC – 10 KHz
Baseline wander	15% of V_{ECG}^{p-p}	continuous	Low frequency

Although most filtering for artifact removal is performed in a digital fashion, the performance of the artifact removal methodologies is strongly dependent of the windowing technique [7, 8]. This work investigates the analog approach to perform filtering or artifact removal. In this work we propose a methodology to adapt the analog filter parameters for artifact removal in biomedical signals. Artifact removal is illustrated on the case of ECG. An ECG unit is illustrated in figure 1 and is explained as follows. The cardiac cycle

Manuscript received July 14, 2015; September 1, 2015

consists of a sequence of two phases, namely the diastole and the systole. In-between heartbeats, the heart is in diastolic rest, therefore stands the rather flat section in the ECG signal. During systole, the atria contract causing the depolarization of the muscle cells, while the ventricles relax. Accordingly, the P wave stands for atrial depolarization. Muscle contraction propagates towards the ventricles, and therefore the QRS complex stands for the ventricular depolarization. On heart muscle relaxation, the heart cells are re-polarized, thus the T wave stands for ventricular re-polarization [1].

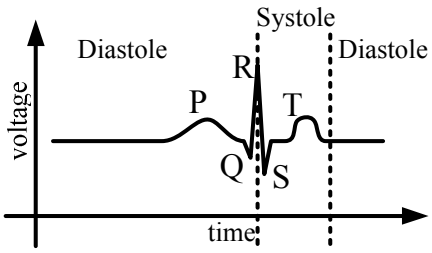

Figure 1. Illustration of an ECG unit.

In order to have a correct diagnosis, the PQRST waves must be clearly visible on the ECG, therefore artifact suppression is mandatory. The block diagram of the ECG analog interface with adaptable filter parameters developed in this work for artifact reduction is illustrated in figure 2. The instrumentation amplifier output is investigated in order to characterize the present artifacts. Next, the analog filter parameters are determined in order to suppress the artifacts. Overall, the block diagram from figure 2 resembles a feed-forward control loop [1, 2].

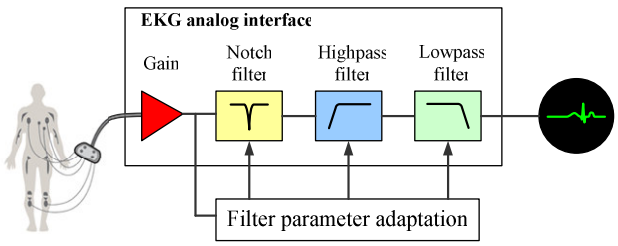

Figure 2. Block diagram of the ECG analog interface with adaptable filter parameters.

This article is organized as follows. Section 2 describes the electronic tunable feature implemented on a Kerwin-Huelsman-Newcomb (KHN) biquad in order to deploy the ECG analog front-end with parameter programmability. Next, Section 3 describes the proposed analog filter parameter adaptation methodology for artifact removal. Section 4 presents simulation results to validate the tunable analog filter and the parameter adaptation methodology. Conclusions are finally drawn.

II. THE ELECTRONICALLY TUNABLE ANALOG FILTER FOR ARTIFACT REMOVAL

The purpose of filtering the biomedical signals is mainly the suppression of the DC component, noise, signal parasitics, etc. This section presents an electronically tunable Gm-C implementation of the KHN biquad, which will be used for artifact reduction in biomedical signals.

The electrical schematic of the operational transconductance amplifier (OTA) is illustrated in Figure 3 and is explained as follows.

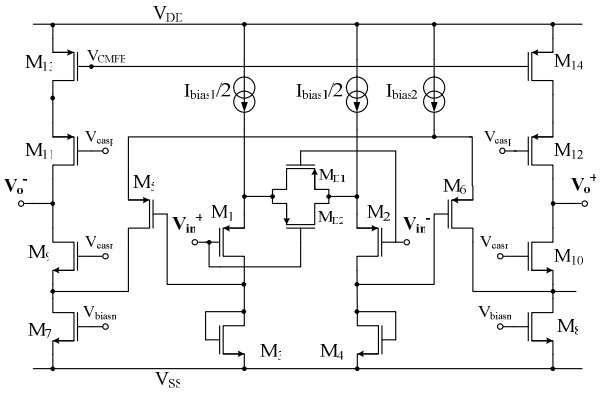

Figure 3. Electrical schematic of the electronically tunable OTA.

The OTA resembles a cascade of two transconductors, as formerly illustrated by Hung et al [9]. The first transconductor consists of input differential pair M_1-M_2, biased with DC current source I_{bias1}, and loaded with diode-connected transistors M_3-M_4. Transistors M_{D1}-M_{D2} biased in the linear region implement source degeneration for transconductor linearization [10]. Accordingly, source degeneration transistors contribute a linearization factor

$$n = 1 + \frac{\beta_1}{4\beta_{D1}} \tag{1}$$

where β_1 is the aspect ratio of the input transistors and β_{D1} is the aspect ratio of the degeneration transistors [10]. The output of the first stage is applied to the input of a folded-cascode OTA, implemented with input transistor pair M_5-M_6, biased with DC current source I_{bias2} and loaded with folded-cascode load M_7-M_{14}.

In this deployment, transistors M_3-M_6 implement a translinear loop [9]. Assuming above threshold operation, the translinear loop is described by equation

$$\sqrt{\frac{I_3}{k_n\left(W/L\right)_3}} + \sqrt{\frac{I_5}{k_p\left(W/L\right)_5}} = \sqrt{\frac{I_4}{k_n\left(W/L\right)_4}} + \sqrt{\frac{I_6}{k_p\left(W/L\right)_6}} \tag{2}$$

The translinear loop was designed such that pMOS transistors M5-M6 compensate the difference in nMOS and pMOS factors kappa. Accordingly, equation (2) can be reduced to

$$\sqrt{I_3} + \sqrt{I_5} = \sqrt{I_4} + \sqrt{I_6} \tag{3}$$

Manipulating equation (3) leads to the expression of the OTA transconductance G_m as a function of the input transistor transconductance $g_{m,in}$, the linearization factor n

expressed in (1), and the OTA bias currents:

$$G_m = \frac{1}{n} \cdot g_{m,in} \cdot 2I_{bias2} \cdot \sqrt{I_{bias2} - I_{bias1}} \qquad (4)$$

To be noticed is that, in comparison to subthreshold operation which yields a linear dependency of the transconductance vs. OTA bias current ratio, as was the case in [9, 11], above threshold operation as is the case in the present work yields a linear transconductance vs. bias current difference dependency.

To enable fully differential operation, the common-mode feedback amplifier illustrated in figure 4 was implemented. The CMFB amplifier is basically implemented with a single-ended amplifier, and operates accordingly. The CMFB amplifier determines the error between the OTA differential output voltage V_o^+-V_o^-, computed on transistor pair M_{CM1}-M_{CM2}, and a common mode reference voltage *Vref*, applied to transistor pair M_{CM3}-M_{CM4}. The error voltage is amplified and applied to the gates of transistors M_{13}-M_{14} in the OTA circuit. Thus, the aim of the CMFB amplifier is to balance the OTA differential output voltage around the DC reference voltage, and to consequently minimize the output offset. Passive capacitances C_1 and C_2 compensate the amplifier for stability of the CMFB loop [12, 13].

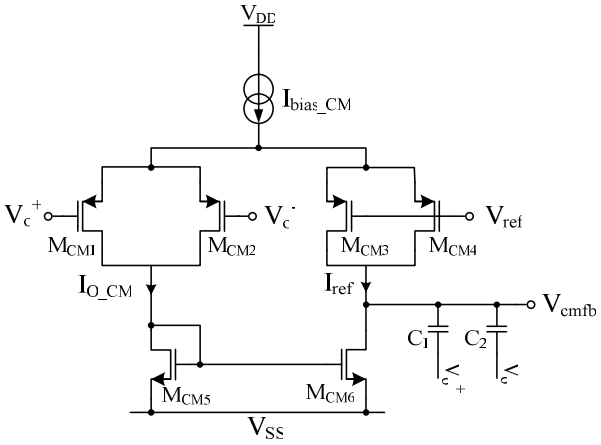

Figure 4. Electrical schematic of the CMFB amplifier.

The proposed OTA was used to implement the KHN biquad illustrated in Figure 5.

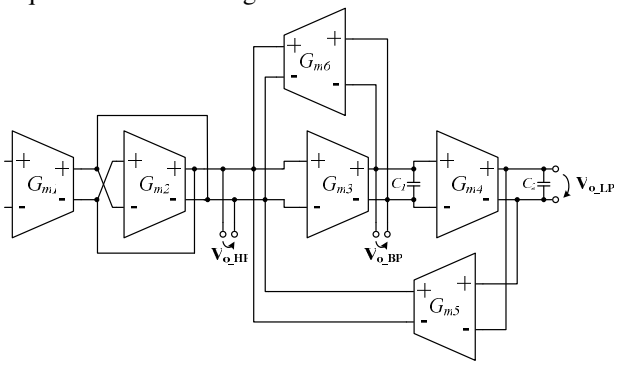

Figure 5. The KHN biquad.

The KHN biquad frequency parameters, namely the filter gain H_0, cutoff frequency f_0 and quality factor Q are expressed as:

$$\begin{cases} H_0 = \dfrac{G_{m1}}{G_{m2}} \\ f_0 = \dfrac{1}{2\pi} \cdot \sqrt{\dfrac{G_{m3} \cdot G_{m4} \cdot G_{m5}}{G_{m2} \cdot C_1 \cdot C_2}} \\ Q = \sqrt{\dfrac{G_{m2} \cdot G_{m4} \cdot G_{m5}}{G_{m3} \cdot G_{m6}^{\,2}}} \cdot \dfrac{C_1}{C_2} \end{cases} \qquad (5)$$

Having the KHN biquad implemented with the proposed OTA enables the electronic tuning of the biquad frequency characteristics as a function of the OTA bias currents respectively, by substituting equation (4) in (5). To be noticed however is that the independent tuning of the KHN biquad frequency parameters requires tuning of multiple OTAs in the KHN structure.

III. THE PROPOSED FILTER PARAMETER ADAPTATION METHODOLOGY

The block diagram of the proposed filter parameter adaptation methodology is illustrated in figure 6 and is explained as follows.

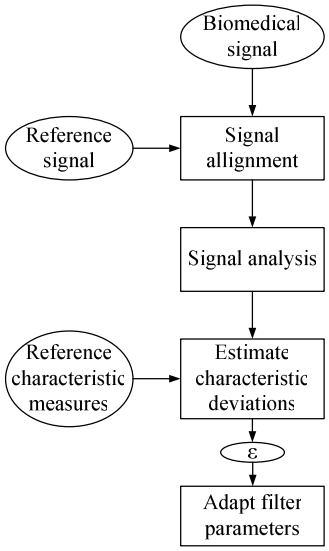

Figure 6. Flow diagram of the proposed filter parameter adaptation methodology.

The filter parameter adaptation methodology was implemented in Matlab, and aims to compute the OTA bias currents for tuning the KHN biquad. Frames of the ECG signal are imported to Matlab and are processed individually. We have experimentally come to the conclusion that best results for artifact reduction were obtained with ECG signal frames consisting of 3 QRS complexes. Therefore, the duration of one frame was set to 5 seconds.

First, the ECG signal frame is aligned with a reference

ECG signal in order to be prepared for further investigation. Signal alignment is performed by shifting the ECG signal with a number of samples determined with the cross-correlation function. The ECG signal frame is then analyzed by means of power spectral density, spectrogram analysis and average power [5]. Next, the computed performance measures are compared to those of the reference ECG signal, and the deviation from the reference performance measures is estimated in the shape of an error value:

$$\varepsilon = \left| perf^{ECG} - perf^{ref} \right| \quad (6)$$

Rather than identifying the artifact and apply specific suppression methods, the aim of the filter parameter adaptation methodology is to minimize the error value expressed in (6), i.e. minimize the deviation between the ECG signal and the reference signal characteristic measures. For this purpose, the filter cutoff frequencies are deviated one step per iteration, assuming a resolution of 100 points per decade. The initial direction of deviation is chosen randomly. Should the error between the ECG signal and the reference performance measures increase, then the direction for cutoff frequency deviation is changed. Otherwise, the deviation is increased an additional step. This procedure is repeated as long as the monotony of error minimization is maintained.

For the initial signal frame to be processed, adaptation of the filter cutoff frequencies starts from the reference filter specifications, which in case of ECG are a highpass cutoff frequency of 0.05Hz and a lowpass cutoff frequency of 100Hz [14]. For all other signal frames, the adaptation of the filter cutoff frequencies starts from the optimal filter parameters of the previous signal frame.

IV. SIMULATION RESULTS

The electronically tunable OTA was designed for above threshold operation with a 3V asymmetric supply. The transistor-level schematic was implemented in LTSpice using a 180nm process. Extensive simulation proves the functionality of the proposed electronically tunable OTA.

The DC characteristics of the linearized OTA are plotted in figure 7 against the DC characteristics with no linearization applied. Dashed line stands for no linearization technique, and solid line stands for source degeneration. According to figure 7, source degeneration extends OTA linearity to $1.8V^{p\text{-}p}$.

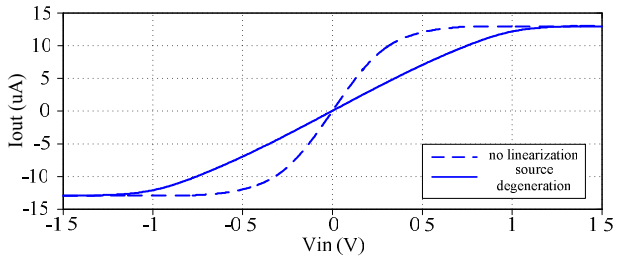

Figure 7. DC transfer characteristics of the OTA.

Electronic tuning of the OTA is illustrated next. In the first simulation scenario, the transconductance is varied as a function of I_{bias1}, as expressed in (4), while I_{bias2} is kept fixed. The resulting DC characteristics are plotted in figure 8 and exhibit a rather non-linear dependency vs. I_{bias1}. The transconductance dependency is however linear with respect to the bias current difference, as expressed in (4).

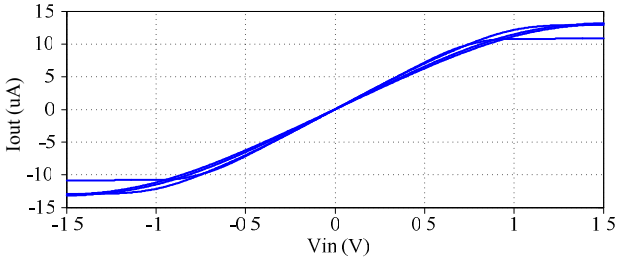

Figure 8. Variation of the OTA transconductance as a function of I_{bias1}.

Variation of the transconductance is varied as a function of I_{bias2}, as expressed in (4), while I_{bias1} is kept fixed. The resulting DC characteristics are plotted in figure 9 and exhibit a linear transconductance dependency vs. I_{bias2}.

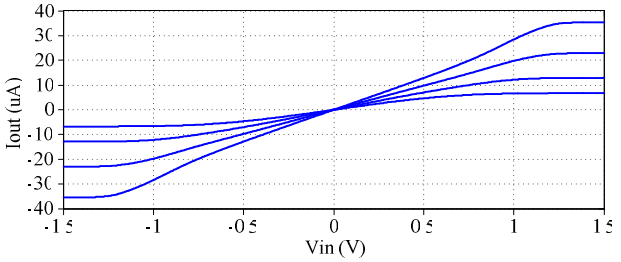

Figure 9. Variation of the OTA transconductance as a function of I_{bias2}.

As can be concluded from figures 8 and 9, due to the linear dependency of the transconductance vs. I_{bias2}, bias current I_{bias2} will be used for tuning the analog filter frequency parameters, while I_{bias1} will only be used if fine-tuning is required.

Electronic tuning of the KHN biquad frequency parameters is presented as follows. For illustration purpose, the highpass biquad output was considered. In the simulation scenarios, parameter variation is performed via I_{bias2}, while I_{bias1} is kept fixed. Variation of the HPF gain as a function of transconductance G_{m1} is plotted in figure 10. Next, variation of the HPF quality factor as a function of transconductance G_{m3} is plotted in figure 11. Finally, variation of the HPF central frequency as a function of transconductance G_{m4} is plotted in figure 12.

Electronic tuning of the KHN biquad frequency characteristics, in terms of gain, cutoff frequency and quality factor, stands for the badpass and lowpass biquad outputs as well.

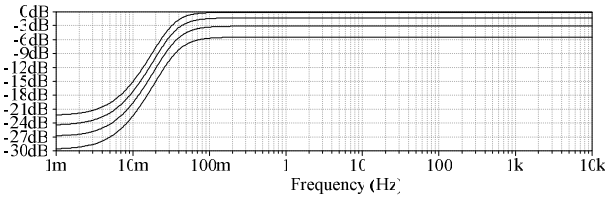

Figure 10. Variation of the HPF gain as a function of G_{m1}.

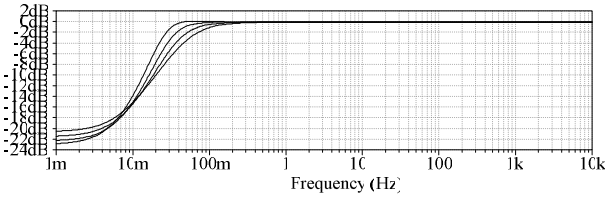

Figure 11. Variation of the HPF quality factor as a function of G_{m3}.

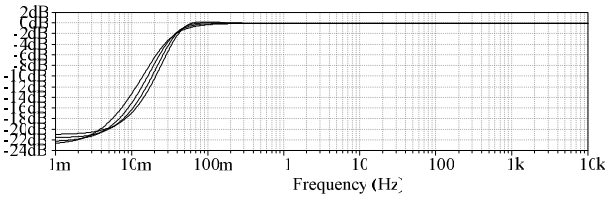

Figure 12. Variation of the HPF central frequency as a function of G_{m4}.

The proposed filter parameter adaptation methodology was implemented in Matlab. Artifact removal is illustrated for the particular case of ECG signal. The proposed filter parameter adaptation methodology operates on real ECG signals recorded with wet Ag/AgCl electrodes, the INA128 instrumentation amplifier and the Analog Discovery acquisition board from Digilent. The test setup for ECG recording is depicted in figure 13.

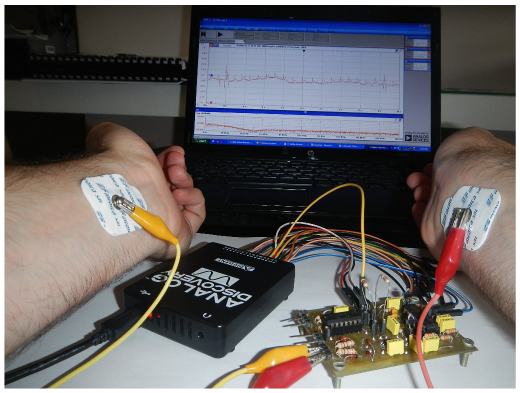

Figure 13. Test setup for the recording of ECG signals.

An ECG signal recorded with the INA128 instrumentation amplifier, exhibiting baseline wander, electrode contact noise and muscle contractions is plotted in figure14. To be noticed is that besides the three artifacts illustrated in figure 14, the ECG signal is also affected by stray interference.

The frequency spectrum of the artifacts is illustrated next, as recorded with the Analog Discovery acquisition board. The frequency spectrum of electrode contact noise is plotted in figure 15. The frequency spectrum of muscle contractions is plotted in figure 16. In both figures 15 and 16, the spectrum of stray interference is visible at frequencies above 100 Hz, where ECG has no spectral components.

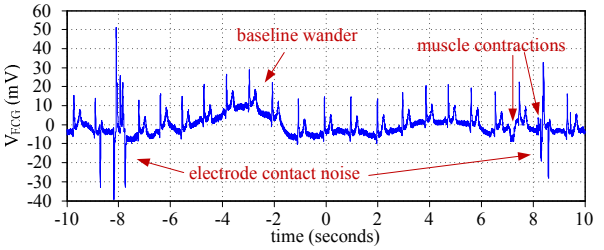

Figure 14. Sample ECG signal exhibiting several artifacts.

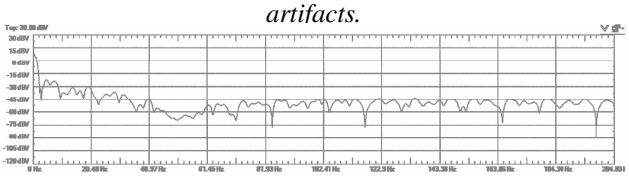

Figure 15. Frequency spectrum of artifact generated from improper electrode contact.

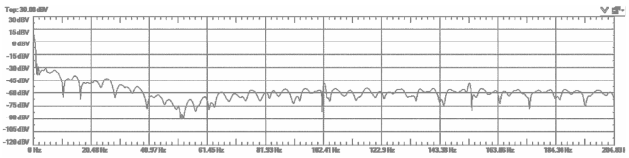

Figure 16. Frequency spectrum of artifacts generated from muscle movement.

Further on, alignment of the ECG signal frame with the reference ECG signal using cross-correlation is illustrated. Figure 17 shows a 5 second frame of the ECG reference signal, the EGC signal recorded with Analog Discovery acquisition board, and their cross-correlation.

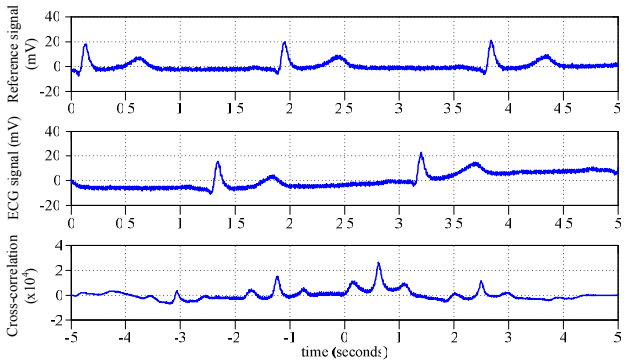

Figure 17. The reference signal, the EGC signal and their cross-correlation.

According to the cross-correlation results plotted in figure 17, a 620 ms shift of the ECG signal is required to align the two signals. The reference signal and the ECG signal, aligned as a result of the cross-correlation maxima, are plotted in figure 18.

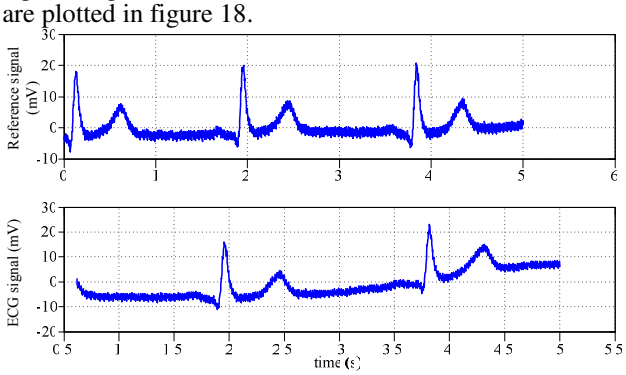

Figure 18. The aligned reference and EGC signals.

The proposed filter parameter adaptation methodology was applied to the ECG signal from figure 14, and the simulation results are plotted in figure 19. As illustrated in figure 19, the magnitude of the artifacts is indeed reduced. The highest impact was on reduction of electrode contact noise, as well as stray interference. To be noticed is however that baseline wander hasn't been suppressed using the proposed filter parameter adaptation methodology.

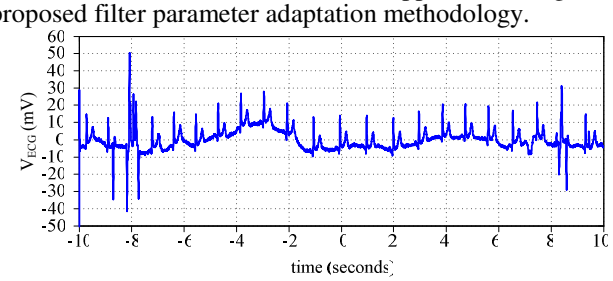

Figure 19. The ECG signal after artifact suppression.

CONCLUSIONS

This article proposed a solution for artifact reduction in bio-medical signals, using tunable analog filters and a filter parameter adaptation methodology.

An electronically tunable OTA was developed for the implementation of the tunable analog filter. The OTA was developed around a cascade of two transconductors, thus implementing a translinear loop which made the transconductance value tunable with the OTA bias currents. The developed OTA was employed to implement a KHN biquad, for filtering the biomedical signals.

A filter parameter adaptation methodology was developed around a feed-forward control loop. Frames of the biomedical signal are analyzed and the analog filter parameters are adapted in order to minimize an error measure which estimates the artifact effects.

Simulation results validate the electronically tunable OTA for implementing tunable analog filters, as well as the proposed filter parameter adaptation methodology for artifact reduction in ECG signals.

As future work, we propose to extend the filter parameter adaptation methodology with the incorporation of computational intelligence techniques to compute the filter parameters, and apply the methodology for artifact reduction in multiple ECG channels.

ACKNOWLEDGEMENTS

This paper was supported by the Post-Doctoral Programme POSDRU/159/1.5/S/137516, project co-funded from European Social Fund through the Human Resources Sectorial Operational Program 2007-2013.

REFERENCES

[1] Rahul Sarpeshkar, *Ultra Low Power Bioelectronics Fundamentals, Biomedical Applications, and Bio-Inspired Systems*, Cambridge University Press, 2010.

[2] B. Râza, A. Râza, P. Faragó, S. Hintea, "Design Illustration Of An EKG Analog Interface Using Genetic Algorithms", *Acta Technica Napocensis - Electronics And Telecommunications*, vol. 55, no. 1, pp.14-19, 2014.

[3] L. Magnelli, F. A. Amoroso, F. Crupi, G. Cappuccino, G. Iannaccone, "Design of a 75-nW, 0.5-V subthreshold complementary metal–oxide–semiconductor operational amplifier", *International Journal of Circuit Theory and Applications*, vol. 42, no. 9, pp. 967–977, 2014.

[4] K. T. Sweeney, H. Ayaz, T. E. Ward, M. Izzetoglu, S. F. McLoone, B. Onaral, "A Methodology for Validating Artifact Removal Techniques for Physiological Signals", *IEEE Transactions on Information Technology in Biomedicine*, vol. 16, no. 5, pp. 918-926, 2012.

[5] S. L. Joshi,R. A. Vatti, R. V. Tornekar, "A Survey on ECG Signal Denoising Techniques", *2013 International Conference on Communication Systems and Network Technologies (CSNT)*, pp. 60 – 64, 2013.

[6] M. Srinivasulu, K. C. Reddy, "Novel Method to Find the Parameter For Noise Removal from Multi-Channel ECG Waveforms", *International Journal of Research in Engineering and Technology*, vol. 3, no. 2, pp. 395-401, 2014.

[7] F. Strasser, M. Muma, A. M. Zoubir, "Motion Artifact Removal in ECG Signals Using Multi-Resolution Thresholding", *20th European Signal processing Conference (EUSIPCO 2012)*, pp. 899-903, Bucharest, Romania, 2012.

[8] R. P. Narwaria, S. Verma, P. K. Singhal, "Removal of Baseline Wander and Power Line Interference from ECG Signal - A Survey Approach", *International Journal of Electronics Engineering*, vol. 3, no. 1, pp. 107– 111, 2011.

[9] C. –C. Hung, I. Halonen, M. Ismail, V. Porra, "Micropower CMOS Gm-C Filters for Speech Signal Processing," *IEEE International Symposium on Circuits and Systems*, Hong Kong, 1997, pp. 1972-1975.

[10] P. Farago, L. Festila, S. Hintea, G. Csipkes, D. Csipkes, P. Soser, "A Transistor-Level Reconfigurable Circuit for Rapid Transconductor Design and Testing", *ELEKTRONIKA IR ELEKTROTECHNIKA*, vol. 117, no. 1, pp. 99-104, 2012.

[11] P. Faragó, C. Faragó, R. Groza, S. Hintea, "An Evolutionary Optimization Methodology of a Low-Power Programmable Cochlear Implant", 38th International Conference on Telecommunications and Signal Processing (TSP), Prague, Czech Republic, July 9-11, 2015.

[12] D. Csipkes, G. Csipkes, P. Farago, H. Fernandez-Canque, S. Hintea, "An OTA-C field programmable analog array for multi-mode filtering applications", *13th International Conference on Optimization of Electrical and Electronic Equipment (OPTIM2012)*, pp. 1176 – 1182, 2012.

[13] P. Farago, D. Bogăţeanu, E. Ceuca, C. Moisă, S. Hintea, "Device mismatch analysis and effect compensation in fundamental analog cells", *2013 36th International Spring Seminar on Electronics Technology (ISSE)*, pp. 280 – 285, 2013

[14] C.-C. Huang, C. Tung, S.-H. Hung, J.-F. Chung, L.-D. Van, C.-T. Lin, "Front-end amplifier of low-noise and tunable BW/gain for portable biomedical signal acquisition", *IEEE International Symposium on Circuits and Systems*, pp. 2717–2720, 2008.